

Diagnostic of the Decomposition of Sulphur Hexafluoride (SF₆) in Gas-Insulated Equipment, Due to Partial Discharges, Using Hollow Carbon Nanotubes

T. CHENAF^{a,*}, B. ZEGNINI^a AND A. BENGHIA^b

^aLaboratoire d'étude et développement des matériaux semi-conducteurs et diélectriques,

Amar Telidji University of Laghouat, BP 37G, Laghouat 03000, Algeria

^bLaboratoire de physique des matériaux, Amar Telidji University of Laghouat, BP 37G, Laghouat 03000, Algeria

Sulphur hexafluoride, SF₆ gas has excellent physical and chemical properties and insulation arc extinction performance. It has been widely used in electric power systems and other electrical equipment due to such advantages, as compact size and high reliability. SF₆, can be decomposed into different gases, when the equipment exhibits arc discharge, local heating of contactor, and partial discharge. It is important to detect decomposition of insulating gas SF₆, caused by partial discharges for gas-insulated switchgear. Partial discharge in gas-insulated switchgear can lead to the generation of multiple decomposition products of SF₆, and the detection and analysis of these decomposition products is important for fault diagnosis. The detection of decomposition components is needed to maintain on-line running state monitoring. Recently, interest in carbon nanotubes has been rapidly growing in various scientific and engineering fields, because of their faster response, higher sensitivity, lower operating temperature and a wider variety of detectable gas. In this paper, a molecular dynamics simulation software package, Materials Studio, is used to model accurately the processes by which single-walled carbon nanotubes could detect studied gases. All calculations were performed using the DMol³ module of the Materials Studio. We compute the preferential adsorption sites, bonding configurations, and adsorption geometry for molecular adsorption. Results of analysis of electrical characteristics reveal that SWCNTs show different responses to the decomposed gases.

DOI: [10.12693/APhysPolA.132.1176](https://doi.org/10.12693/APhysPolA.132.1176)

PACS/topics: Gas insulated switchgear, decomposition gases, carbon nanotube, Material Studio (MS), DMol³ module, adsorption, graphene sheets.

1. Introduction

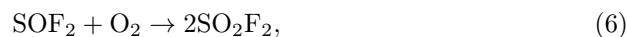
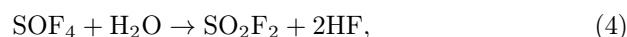
With the development of the power industry, gas-insulated switchgear (GIS) has become more widely used in the power systems for its advantages of high reliability, small volume, and simple maintenance. Sulfur hexafluoride (SF₆) is used in GIS for its good insulating performance and arc extinction properties. However, SF₆ gas has harmful drawbacks, potentially affecting the nature, by its contribution to the greenhouse effect, and the equipment, after its decomposition into such products as SF₄, F₂, SOF₂, SO₂F₂, SOF₄, SO₂ and HF [1]. The decomposition of SF₆ gas in GIS occurs due to construction defects and impurities via the partial discharge (PD) process.

Carbon nanotubes (CNT) have received considerable attention in the field of electrochemical sensing, due to their unique structural, electronic and chemical properties, such as, for instance, unique tubular nanostructure, large specific surface, excellent conductivity, modifiable sidewall and good biocompatibility [2–9]. Recently, interest in CNT has been rapidly growing in various scientific and engineering fields because of their fast response [10–13], higher sensitivity, lower operating temperature and a wider variety of detectable gases [14].

However, the PD-generated decomposition gas species, which generate the CNT gas sensor response, have not been yet identified. In this paper we propose a PD detection method using CNT.

2. The mechanism of SF₆ decomposition during DP

The decomposition of SF₆ during PD is highly complex, involving complicated physical and chemical processes. The basic decomposition processes are as follows: firstly, SF₆ molecules decompose during PD, into SF₅, SF₄, SF₃ and F; these decomposition components then react with trace water, trace oxygen or insulating materials in the GIS to produce SOF₄, SOF₂ and SO₂F₂ chemical products [15]. The relevant chemical equations are as follows:



The mechanism of decomposition of SF₆ gas depends on the nature of the electrical stress and, therefore, on the place where it occurs. It was found [3], that under partial discharges, products of discharge differ depending on

*corresponding author; e-mail: nchenaf@hotmail.fr

the region inside the GIS equipment, where the discharge occurs. These regions are near the electrodes, between the electrodes or further region, named as glow luminescent region, ion drift region and the region of the main gas volume (see Fig. 1).

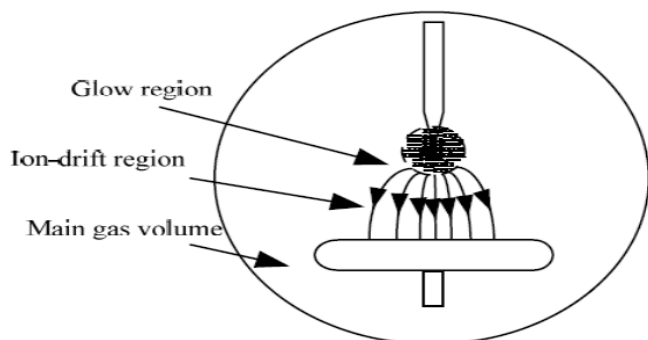


Fig. 1. Model of the decomposition mechanism of SF_6 gas under partial discharge [3].

The detection of discharge products is possible using single wall carbon nanotubes SWNTs, which have a high surface adsorption capacity and good conductivity. The placement of a nanotube sensor in the discharge chamber with SF_6 gas and measurement of its resistance have allowed us to determine the sensitivity of the detector [16].

3. Simulation and computation details

In this study we have used Material Studio (MS) simulator, developed by the American company Accelrys. The MS software package, based on density functional theory, has been used extensively in the field of material science. Density functional theory is based on ab initio quantum mechanics to study the electronic structure of multi-electron systems. DMol³ module was used to prove the ability of nanotubes to detect the studied gases.

To achieve good results the accurate description of the geometric structures of electronic components used in the study (nanotubes and molecules) has to be obtained. A large number of optimizations of the structure were carried out using different functionals: DFT (density functional theory) (GGA-PBE) generalized gradient approximation-Perdew-Burke-Ernzerhof [17] and corrections DFT-D GGA-PBE-Grimme (GGA-PBE-G06).

Carbon nanotubes are assumed to be rigid and dimensionally stable. In our simulations we have set the carbon atoms to avoid their interaction and deformation. A portion of a nanotube, consisting of 68 carbon atoms, is selected as the simulation model.

Procedure used in this study, after comparison of approaches, is to construct nanotube, molecule of SF_6 gas and its decomposition products, optimize geometry of each molecule individually with and without the nanotube, and to find their corresponding energies. Essentially in this article we have introduced the concept of (DFT-D) that considers the Van der Walls bonding [18].

The positions of the molecules with respect to the nanotube were randomly chosen before optimizing geometries. Finally an analysis of electron density, distances, energy and transfer of charges was made in order to conclude modifications to the nanotube characteristics, to confirm its efficacy as a detector, sensitive to the decomposition products during the partial discharge.

After selection of the approaches we have built molecules from the decomposition of parent SF_6 molecules Fig. 2. Then we have built systems including the chosen molecules and the nanotube Fig. 3.

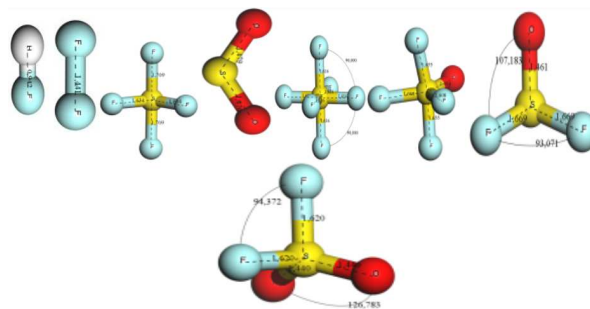


Fig. 2. Optimized molecules, created during PD: HF , F_2 , SF_4 , SO_2 , SF_6 , SOF_4 , SOF_2 , SO_2F_2 .

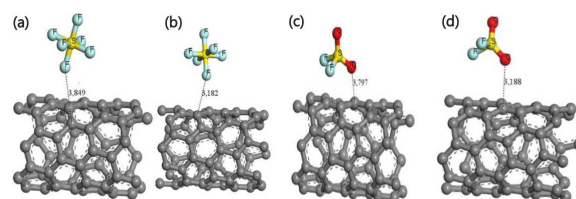


Fig. 3. Optimization of molecule-SWNT systems, with provided distances (\AA). (a) SF_6 -SWNT DF; (b) SF_6 -SWNT DFT-D; (c) SO_2F_2 -SWNT DFT; (d) SO_2F_2 -SWNT DFT-D.

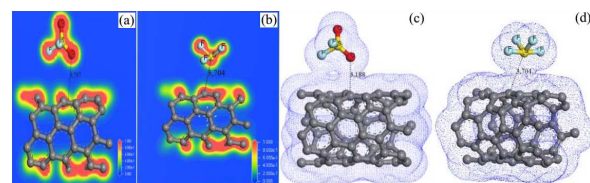


Fig. 4. Electronic density of the system of molecule-SWNT. 2D (a) SO_2F_2 , (b) SF_4 ; 3D (c) SO_2F_2 , (d) SF_4 .

4. Results and discussion

We will discuss the optimization distances, adsorption energies, the charge transfer between molecules and nanotubes, E_{gap} and electronic density.

4.1. Optimization energies and distances

The optimized distances range from 2.204 \AA for F_2 molecule (fluorine) to 4.514 \AA for SO_2 molecule (sulfur

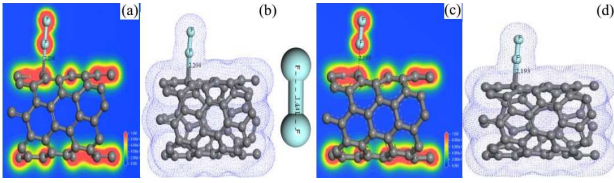


Fig. 5. Electronic density of the system of F_2 -SWNT, (a), (c) 2D; (b), (d) 3D in DFT and DFT-D.

dioxide), according to DFT method, and from 2.193 Å for F_2 molecule to 3.445 Å for molecule SO_2 , according to DFT-D. There is a decrease in the distance in DFT-D method.

TABLE I

Energies, distances and adsorption energies of molecule-SWNT systems, calculated using DFT and DFT-D methods.

Systems	Energy DFT (Ha)	Energy DFT-D (Ha)	Dist. optim. DFT [Å]	Dist. optim. DFT-D [Å]	E_{ads} [eV] DFT	E_{ads} [eV] DFT-D
SWCNT	-2435.001	-2435.115	-	-	-	-
SF ₆ -NT	-3431.808	-3431.925	3.849	3.182	-1.061	-1.1
HF-NT	-2535.401	-2535.516	3.079	2.947	-0.32	-0.353
F ₂ -NT	-2634.452	-2634.441	2.204	2.193	+0.979	+4.381
SF ₄ -NT	-3232.778	-3232.895	3.704	3.373	-15.29	-15.35
SOF ₄ -NT	-3307.387	-3307.504	3.604	3.202	-1.061	-0.952
SO ₂ F ₂ -NT	-3183.561	-3183.678	3.797	3.188	-15.27	-15.29
SOF ₂ -NT	-3107.854	-3107.971	3.819	3.460	-1.061	-1.115
SO ₂ -NT	-2983.438	-2983.553	4.514	3.445	-1.088	-1.115

4.2. Energy adsorption

Negative energy means that the adsorption process is exothermic and can occur spontaneously and that there is always an interaction between the molecules and SWCNT, this energy is calculated using Eq. (8) [19]. This is the energy required to pull away the molecule attached to the nanotube. We note that it is positive only for F_2 molecule, 0.979 eV in DFT and 4.381 eV in DFT-D, which explains its attachment to the nanotube.

$$E_{ads} = E_{Molecule-SWNT} - E_{SWNT} - E_{Molecule}. \quad (8)$$

4.3. The charge transfer

Each isolated molecule has a zero charge, but once beside the nanotube, due to inter-atomic attraction the charge is transferred between the molecule and the CNT, with the exception of molecules of SF_6 and SF_4 which do not display such interaction in DFT and DFT-D, see Table II. This charge transfer is important for F_2 molecule (-0.3e). This molecule has reacted with the nanotube through the creation of a bond (Fig. 5b).

For other molecules there is a transfer of charge. It must be taken into consideration for the molecules that can change the electrical characteristics of the nanotube.

The signs of the charge gives us an idea of the direction of transfer.

The change in charge distribution should be known. Therefore, charge transfer is calculated using the Milliken population analysis, defined as the charge variation of isolated gas molecules upon adsorption [20]. If this charge is positive, this indicates that the charge is transferred from the molecule to the nanotube surface. The binding distance is defined as the nearest distance between the molecule and the surface [21].

TABLE II

Optimization energies and charges of molecules interacting with SWNT, calculated using DFT and DFT-D.

Molecules	Energy DFT [Ha]	Energy DFT-D [Ha]	Charge DFT (e)	Charge DFT-D (e)
SF ₆	-996.768	-996.770	0.000	0.003
HF	-100.388	-100.388	0.004	0.007
F ₂	-199.487	-199.487	-0.300	-0.307
SF ₄	-797.215	-797.216	0.000	-0.001
SOF ₄	-872.347	-872.350	0.001	0.004
SO ₂ F ₂	-747.999	-748.001	0.002	0.004
SOF ₂	-672.814	-672.815	0.001	0.002
SO ₂	-548.397	-548.397	0.003	-0.013

4.4. Energy gap E_{gap}

The energy gap E_{gap} of adsorption structure can be calculated through the energy levels of the HOMO and LUMO, defined as $E_{gap} = |E_{HOMO} - E_{LUMO}|$ [21]. The calculated adsorption parameters of the molecules are shown in Table III.

Comparing the E_{gap} of nanotube with those of molecules we did not notice much change for the molecule SF_6 , SF_4 and SO_2F_2 whatsoever in DFT or DFT-D. However, for other molecules it decreased, which means that the conductivity does not change much for molecules SF_6 , SF_4 and SO_2F_2 .

TABLE III

Energy gap E_{gap} of molecule-SWNT systems.

Systems	HOMO		LUMO		E_{gap} [eV]	E_{gap} [eV]
	DFT	DFT-D	DFT	DFT-D	DFT	DFT-D
SWCNT	-6.017	-	-5.956	-	0.061	-
SF ₆ -SWCNT	-5.972	-5.976	-5.970	-5.974	0.002	0.002
HF-SWCNT	-5.783	-5.782	-5.781	-5.779	0.002	0.003
F ₂ -SWCNT	-6.114	-6.125	-6.107	-6.118	0.007	0.007
SF ₄ -SWCNT	-6.208	-6.213	-6.143	-6.148	0.065	0.065
SOF ₄ -SWCNT	-5.962	-5.958	-5.960	-5.955	0.002	0.003
SO ₂ F ₂ -SWCNT	-6.146	-6.138	-6.079	-6.071	0.067	0.067
SOF ₂ -SWCNT	-6.051	-6.065	-6.048	-6.046	0.003	0.001
SO ₂ -SWCNT	-5.907	-5.973	-5.906	-5.971	0.001	0.002

4.5. Electronic density of states

From Fig. 6b we found that the total electronic density of states of SF_6 molecules systems, and the HF, F_2 ,

SO_2F_2 , SO_2 systems are similar to that of the SWNT, however in Fig. 7 these characteristics are different for SF_4 and SO_2F_2 molecules, due to the change of the electronic properties of SWNTs, so they can be easily detected by the nanotube. Figure 6a represents the curves of all molecules with that of SWNT.

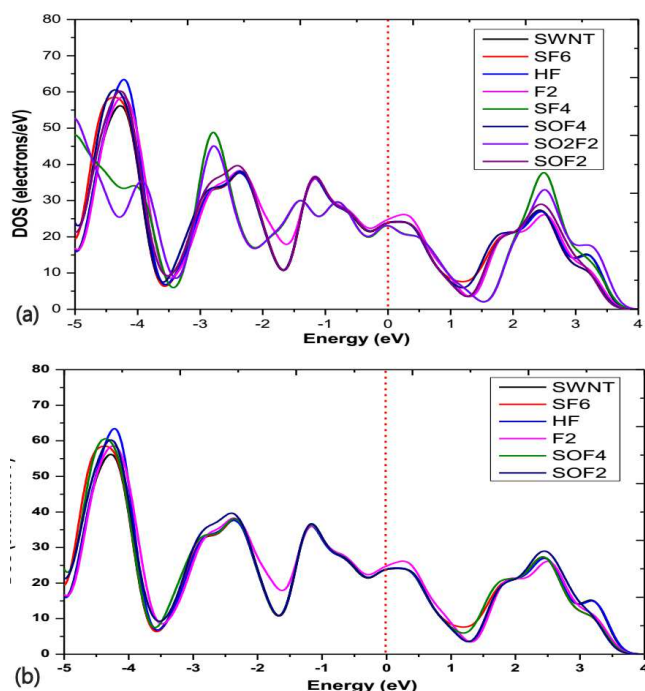


Fig. 6. Electronic density of states for molecule-SWNT systems, (a) with all molecules, (b) with SF_6 , HF, F_2 , SF_4 , SO_2F_2 .

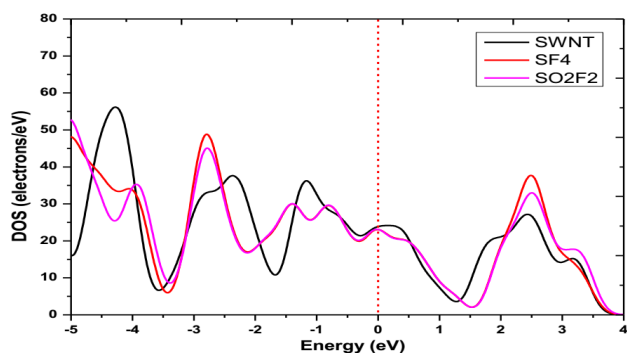


Fig. 7. Electronic density of states for molecule-SWNT systems with SF_4 and SO_2F_2 .

This result reveals that the SWNT is able to adsorb and detect the molecules of SF_4 (sulfur tetrafluoride) and SO_2F_2 (sulfuryl fluoride) easily. It can be seen from the curves and also from the values of E_{ads} of SF_4 and SO_2F_2 , respectively -15.292 eV and -15.265 eV.

Molecule F_2 forms a bond with the SWNT, which means that chemical adsorption occurs. E_{ads} for this molecule is very important. It should be noted that the

the difference between 0.979 eV in DFT and 4.381 eV in DFT-D is related with taking into consideration the Van der Waals interaction.

Other molecules have lesser effects than the molecules of SF_4 and SO_2F_2 , but if we consider that the gas may contain a large number of molecules from the decomposition of the SF_6 , the electrical characteristics (conductivity and sensitivity) may change. Analysis reveals that SWCNTs show different responses to five investigated gases. The calculated effects, regardless of their magnitudes, can also be amplified by electronic circuits, to be detectable. Thus every kind of molecule has a unique effect on the CNT, acting as a fingerprint, which can be read using the CNT.

5. Conclusions

In this paper, MS software, based on density functional theory, was used to simulate the adsorption of the five major decomposition products of SF_6 , which are created during PD. Single-wall carbon nanotube chemical sensors have extensive application in gas detection. SWCNTs can achieve high precision and selectivity by different doping methods. We compute the preferential adsorption sites, bonding configurations, and adsorption geometry for molecular adsorption. Results of analysis of electrical characteristics reveal that SWCNTs show different responses to the decomposed gases.

Acknowledgments

The authors gratefully acknowledge the computing equipment and Material Studio software (Dmol³ module) support from Laboratoire de Physique des Matériaux, (LPM) Amar Telidji University of Laghouat, Algeria.

References

- [1] F. Chu, *IEEE Trans. Electr. Insul.* **EI-21**, 693 (1986).
- [2] A. Bahari, M. Amiri, *Acta Phys. Pol. A* **115**, 625 (2009).
- [3] R. Van Brunt, J. Herron, *Phys. Scripta* **T53**, 9 (1994).
- [4] N. Yuca, N. Karatepe, F. Yakuphanoglu, Y. Gursel, *Acta Phys. Pol. A* **123**, 352 (2013).
- [5] D. Krychowski, S. Lipinski, *Acta Phys. Pol. A* **113**, 545 (2008).
- [6] L. Chico, H. Santos, A. Ayuela, M. Pelc, W. Jaskolski, *Acta Phys. Pol. A* **114**, 1085 (2008).
- [7] H. Choi, J. Kim, C. Lee, *Acta Phys. Pol. A* **115**, 1078 (2009).
- [8] D. Krychowski, S. Lipinski, *Acta Phys. Pol. A* **113**, 645 (2008).
- [9] W. Jaskolski, A. Stachow, L. Chico, *Acta Phys. Pol. A* **108**, 697 (2005).
- [10] K. Rezouali, M. Belkhir, *Acta Phys. Pol. A* **113**, 713 (2008).

- [11] K. Milowska, M. Birowska, J. Majewski, *Acta Phys. Pol. A* **116**, 841 (2009).
- [12] S. Ghaziof, M. Mehdikhani-Nahrkhalaji, *Acta Phys. Pol. A* **131**, 428 (2017).
- [13] Ö. Mermer, S. Okur, F. Sümer, C. Özbek, S. Sayın, M. Yılmaz, *Acta Phys. Pol. A* **121**, 240 (2012).
- [14] P. Kašmierczak, J. Binder, K. Boryczko, T. Ciuk, W. Strupiński, R. Stępniewski, A. Wysmołek, *Acta Phys. Pol. A* **126**, 1209 (2014).
- [15] Z. Li, S. Chen, S. Gong, B. Feng, Z. Zhou, *Computat. Theor. Chem.* **1088**, 24 (2016).
- [16] X. Zhang, F. Meng, B. Yang, *IEEE Trans. Dielectrics Electric Insul.* **20**, 2246 (2013).
- [17] J.P. Perdew, K. Burke, M. Ernzerhof, *Phys. Rev. Lett.* **77**, 3865 (1996).
- [18] J. van de Streek, M.A. Neumann, *Acta Crystallograph. B* **70**, 1020 (2014).
- [19] X. Zhang, J. Zhang, J. Tang, B. Yang, *J. Computat. Theor. Nanosci.* **9**, 1096 (2012).
- [20] S. Peng, K. Cho, *Nano Letters* **3**, 513 (2003).
- [21] X. Zhang, Q. Chen, J. Tang, W. Hu, J. Zhang, *Scientific Rep.* **4**, 4762 (2014).